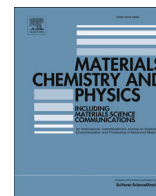




Contents lists available at ScienceDirect

Materials Chemistry and Physics

journal homepage: www.elsevier.com/locate/matchemphys

Synthesis and characterization of epoxy encapsulating silica microcapsules and amine functionalized silica nanoparticles for development of an innovative self-healing concrete

G. Perez ^{a,*}, E. Erkizia ^b, J.J. Gaitero ^b, I. Kaltzakorta ^b, I. Jiménez ^a, A. Guerrero ^a

^a Institute of Construction Science "Eduardo Torroja", CSIC, c/ Serrano Galvache, 4, E-28033 Madrid, Spain

^b Tecnalia, Materials, Sustainable Construction Division, c/ Geldo, Edificio 700, Parque Tecnológico de Bizkaia, 48160 Derio, Spain

ARTICLE INFO

Article history:

Received 7 January 2015

Received in revised form

17 July 2015

Accepted 22 August 2015

Available online xxx

Keywords:

Composite materials

Chemical synthesis

Chemical techniques

Microstructure

ABSTRACT

Silica microcapsules encapsulating an epoxy compound (CAP) and silica nanoparticles functionalized by an amine group (NS) are synthesized to be used as self-healing system for smart cementitious composites. The innovative character of this system comes from the use of silica shell microcapsules to improve the durability and compatibility with the cement and from the use of functionalized nanosilica to obtain an amine functionalized cementitious matrix. Characterization of the particles indicates that they are amorphous and possess a proper morphology and size to be considered as additions to cement. The stability of the epoxy compound inside the microcapsules and the presence of amine groups bonded to silica nanoparticles are also confirmed. Moreover, NS shows a pozzolanic activity superior to that of the silica fume used as reference, while CAP is to a high degree stable upon reaction with lime. The results confirm that the synthesized particles are a suitable starting point to address the development of a smart self-healing concrete.

© 2015 Published by Elsevier B.V.

1. Introduction

Cement composites are one of the most important materials in the modern world. These materials show good mechanical properties and they are relatively inexpensive, both of which make them ideal for use in large quantities. However, during the lifetime of structures, they are subjected to several actions that invariably form cracks. These cracks often lead to durability problems that undermine structural integrity, reduce their performance and result in the need of costly repair works. In order to improve the long-term durability of cement composites, material scientists have recently challenged the traditional way of designing structures –which aims to prevent damage– by developing smart materials that mimic natural living materials and their ability to adapt and respond to their environment by self-repairing. Even though a number of approaches to self-healing materials had been explored before, it was really White

et al. who revolutionized this field with their 2001 Nature article "Autonomous Healing of Polymer Composites" [1], by using polymeric microcapsules encapsulating a curing compound as a self-healing system for an epoxy resin matrix. After publication of this article, research into self-healing spread to different materials, including cement composites [2–8]. In general three different approaches have been explored [9]: the introduction of vascular systems with curing agents mimicking human veins, the maximization of the intrinsic healing capacity of the matrix mainly by the activation of unreacted material within the matrix, and the addition of repairing component sequestered into capsules. Although some researchers are working on the use of bacteria as healing agents, polymers are still the most widely studied healing compounds for cementitious materials [4]. Polymeric systems consist almost invariably of two components and reaction only takes place when they meet. In some cases, one of the components is just water or air and the main difficulty relies on keeping them away from the polymer to prevent premature reaction. Also, and because of their reactivity with water and air, these type of polymers are more complex to encapsulate (in dry and inert environment). On the contrary, when the second

* Corresponding author.

E-mail address: gperezaq@ietcc.csic.es (G. Perez).

component is another chemical compound except water or air, it must also be introduced into the matrix. Of the whole range of polymers available, epoxy resin is one of the adhesive compounds studied for self healing applications [10]. Several epoxy monomers have already been successfully encapsulated due to their good emulsivity in aqueous environments [11,12]. However, the incorporation of suitable hardeners is rather challenging [10] and for the self-healing system to work it requires that both materials (epoxy and hardener compounds) should be available nearby to meet and react when and where the microcrack occurs. In addition to the chemical compatibility with the epoxy resin, the long term and thermal stability of the shell of the microcapsules, generally made of organic compounds, are strongly influenced by the corrosive hardener [13].

Taking the above into account we are developing an innovative self-healing system for cement-based materials based on a two-component epoxy-amine curing agent but with several different characteristics from other epoxy-amine healing systems found in the literature [7,13]. On one hand, and to overcome the possible shell degradation in the long run, the epoxy compound in our system is encapsulated in silica shell microcapsules unlike in some other studies where the epoxy was encapsulated in organic microcapsules [7]. Silica is known to have high chemical resistance and good mechanical strength [14] which is also an important characteristic in order to withstand the mixing process for the preparation of cementitious materials. Furthermore, since the shell is made of silica we expect it will have good interaction with the cementitious matrix, whose major component is the calcium silicate hydrate (C–S–H gel). This is an important feature because we want the microcracks, when they form, to also break the microcapsules instead of going around them. Yang et al. [5] have also used silica shell to encapsulate both parts of the curing system, which in their case was the monomer methylmethacrylate with triethylborane as a catalyst. They indicated that a strong bonding was expected between the silica microcapsules and the cement matrix because the silica of the shell could participate in pozzolanic reactions with the portlandite of the cement matrix.

On the other hand, in our self-healing system, we have also brought in another innovative and, to the best of our knowledge, unique approach, which is the way the second component is introduced into the matrix. The amine group, which is necessary to harden the epoxy resin, is not introduced encapsulated to maintain it isolated from the matrix [7] but is intended to become part of it. To do so, we have developed amine functionalized silica nanoparticles that are added to the cementitious material during the mixing process. Thanks to the expected large reactivity of the nanoparticles, they would induce a pozzolanic reaction that would result in the production of an amine functionalized cementitious matrix. Once a propagating crack breaks the microcapsules, the epoxy compound would be liberated and meet the amine functional groups that are tethered in the silicate chains of the matrix. The two components of the adhesive would then react and the hardened epoxy would end up permanently attached to the matrix, thus sealing the crack.

In this article the synthesis process of both types of particles, together with their characterization, will be described. Furthermore, and as a first step toward developing a self-healing smart concrete, their pozzolanic activity will be assessed. As aforementioned, this property is critical because the whole self-healing system relies on the reaction of the additions with the matrix. The results for silica fume (SF) will also be presented for comparative reasons, as this is a pozzolanic addition commonly used by the cement industry [15].

2. Experimental

2.1. Materials

Tetraethoxysilane (TEOS, 98% (GC)), 3-aminopropyltriethoxysilane and ammonium hydroxide (ACT Reagent, 28–30%) were purchased from Sigma–Aldrich. Ethanol (EtOH, 96% v/v PA) and hydrochloric acid (37% chemically pure) were from Panreac and EPOTHIN[®] was bought from Buehler. Solutions of ammonium hydroxide 0.1 M and hydrochloric acid 1 M were prepared for the reaction from the concentrated solutions. Distilled water was used in all cases. Silica fume used as reference material was ELKEM 940U.

2.2. Synthesis of silica microcapsules encapsulating Epothin[®]

The microencapsulation of the material Epothin[®] has been based on the procedure used by Ahn et al. [16]. A sol–gel reaction followed by an oil-in-water emulsion has been used for the synthesis. In a first step a precursor is obtained by hydrolysing 11.2 mL (0.05 mol) of TEOS with water in acidic conditions (pH~2) during 5 h in a reflux at 40 °C. The molar ratio of the reactants used in this first step is 1:4:1:3 × 10⁻³ of TEOS:EtOH:H₂O:HCl. In the next step, 3 mL of Epothin[®] is added to the precursor, followed by 25 mL of water and a mechanical stirrer is used at 600 rpm to form an emulsion. Ammonium hydroxide solution 0.1 M is added to the emulsion drop wise until the pH is around 10. After the addition of NH₄OH a white solid can be seen in the reaction mixture. The suspension of microcapsules is left aging for an hour and the solid is collected by centrifuge. This solid is washed 3 times with water and collected every time by centrifuge and finally dried at room temperature. The yield of microcapsules with Epothin[®] is around 2 g (1.90 g–2.30 g).

2.3. Synthesis of propylamine functionalized silica nanoparticles

The route of synthesis is based on the Stöber method [17] and in this case the tetraethoxysilane is reacted with 3-aminopropyltriethoxysilane in a one pot reaction to obtain the amine functionalization [18]. Ethanol (4 L), water (83.3 mL), tetraethoxysilane (121 mL, 0.542 mol) and 3-aminopropyltriethoxysilane (13.2 mL, 0.0566 mol) are added to a round bottom flask. To this, concentrated ammonium hydroxide (39 mL) is added and the reaction is left stirring for three days. After these three days, a white colloidal dispersion is obtained. The solid is separated from the solvent by centrifuge and decanting. The solid is washed three times with ethanol to remove any reactants and centrifuged and decanted to collect it. The white solid obtained is air dried. The yield of the nanoparticles is around 40 g (35 g–41 g).

2.4. Characterization of synthesized materials

Morphology and elemental composition were studied with a Hitachi S-4800 scanning electron microscope (SEM-EDX) and a FEI Quanta 200 environmental scanning electron microscope that has an energy dispersive X-ray microanalysis (EDX). In the first case, samples were previously coated with a carbon layer to avoid surface charging. In some cases, the results were complemented with dynamic light scattering measurements carried out in a Malvern Zetasizer in order to quantify particle size distribution.

Solid-state ²⁹Si and ¹³C NMR experiments for the aminopropyl silica nanoparticles were performed on a 400 MHz Bruker Advance III, while the solid-state ²⁹Si NMR characterization of the silica microcapsules was carried out on a 300 MHz Bruker Advance DSX300 NMR spectrometer. Infrared transmission spectra (FTIR) of the samples under study were measured in a Nicolet 6700

spectrophotometer in the wavenumber range from 4000 to 400 cm^{-1} . Samples were prepared in the form of pellets, mixing 1 mg of sample with 300 mg of KBr.

The oxide content of the particles was determined by X-ray fluorescence (XRF) using Bruker S8 Tiger equipment. Complementarily, for the determination of the weight loss on ignition (LOI) the samples were subjected to a temperature of 1020 °C for 1 h. X-ray diffraction (XRD) of the particles was performed in a Philips PW 1730 diffractometer with a graphite monochromator and Cu K_α radiation in order to detect the presence of crystalline phases. The samples were prepared in the form of pellets and they were studied by the powder method.

Nitrogen adsorption–desorption isotherms were measured with a Micromeritics ASAP 2010 analyzer. A sample degassing at 50 °C for 24 h was performed previous to every measurement. Specific surface area values were calculated from the isotherm data using the Brunauer–Emmett–Teller (BET) method in a relative pressure range of 0.003–0.3.

Finally, the pozzolanic activity of both additions was determined by an accelerated method [19] in which the samples were placed in contact with a saturated lime solution at 40 °C for 1, 3, 7 and 28 days. After each period, the CaO concentration in the solution was analyzed and the combined lime was obtained by the difference between the concentration in a control saturated lime solution and that found in the solution in contact with the sample.

3. Results and discussion

3.1. Morphological and compositional analysis

The shape and size of the synthesized particles was analyzed by scanning electron microscopy (SEM). The images presented in Fig. 1 correspond to the epoxy containing microcapsules (CAP). In Fig. 1a) an image of several microcapsules can be seen, one of them broken showing their core/shell structure, and in Fig. 1b) its corresponding elemental mapping is included. Silicon from the silica of the microcapsules is shown in blue, carbon from the remnants of the organic compound epoxy in red and aluminium from the stub used to place the sample in green. It has to be underlined that the signal of the carbon is found within the broken microcapsule, verifying that the epoxy resin is properly encapsulated. In the SEM images of Fig. 1c) and 1d) a wide range of diameters may be seen as obtained in the synthesis, with particle size varying from around 180 μm to less than 5 μm , in good agreement with previous results [16,20]. The microcapsules show in general a uniform spherical shape and, although their surface often shows pore-like morphologies (Fig. 1e), no sign of epoxy spreading out through them is observed in SEM images.

The microcapsules were characterized by 90° pulse ^{29}Si NMR and the corresponding spectrum is shown in Fig. 2. Two major peaks can be seen at –100.9 and –111.1 ppm chemical shifts which are due to Q_3 and Q_4 siloxane groups, respectively [21]. There is also another peak at –91.4 ppm which could be assigned to a Q_2 siloxane group. The Q_2 and Q_3 signals indicate that there are silicon atoms in the siloxane groups that are bound to OH groups (two in the case of Q_2 and one in the case of Q_3). This means that not all the hydroxyl groups have condensed to give a Si–O–Si bond.

In the case of the amine functionalized silica nanoparticles (NS) the size of the particles was characterized in the reaction dispersion by dynamic light scattering (DLS). As it can be seen in Fig. 3a), there is a unimodal particle size distribution with a mean diameter of around 150 nm. After the functionalized nanoparticles were isolated by centrifuge, the morphology of the obtained white solid was characterized by SEM (Fig. 3b) and c)). As it can be seen in Fig. 3c) the NS agglomerated in the process of isolating the product, as

expected. In the image, the single NS particles can be perceived clearly, showing an almost spherical shape with a nearly homogeneous diameter below 0.15 μm (150 nm), thus confirming the results obtained by DLS. This value is around an order of magnitude higher than the diameter reported by other authors for silica nanoparticles [22–24]; this difference must be related to the amine functionalization of the nanoparticles considered in this work.

The NS have also been characterized by ^{29}Si solid NMR and by ^{13}C solid NMR in order to confirm the presence of the organic functionalization. The ^{29}Si NMR spectrum of the nanoparticles shows 4 peaks (Fig. 4a)). The peaks at –111.7 ppm and –102.0 ppm can be assigned to Q_4 and Q_3 siloxane groups. As in the case of the silica microcapsules this means that not all the hydroxyl groups have condensed to give a Si–O–Si bond. Furthermore, the nanoparticles show a T_3 peak at –67.9 ppm and a T_2 peak, which can be seen as a shoulder at –62.2 ppm. The latter two signals are due to siloxane groups where the silicon atom, besides being bound to oxygen atoms, is also bound to a carbon atom in an organic group and thus confirm that the silica nanoparticles are functionalized [25].

The ^{13}C NMR spectrum of the NS is shown in Fig. 4b) where the peaks at 9.0 ppm, 21.0 ppm and 42.3 ppm correspond to C_1 , C_2 and C_3 respectively of the aminopropyl group bound to the nanosilica particle [25,26]. The small peaks at 17.7 ppm, 29.1 ppm and 58.4 ppm are due to the carbon atoms of the ethoxy groups that have not been completely hydrolyzed [25]. These results corroborate that the silica nanoparticles are functionalized with an aminopropyl group.

Fig. 5 shows an SEM image obtained for the commercial silica fume (SF) as a reference of morphology and shape of common additions in cementitious materials. The image is similar to that published by Hou and co-workers [22] of silica fume formed by pseudo spherical particles with a diameter significantly inhomogeneous. In this case, the diameters are lower than 0.5 μm (500 nm), intermediate between those observed for CAP and NS particles. In this particular case the silica fume shows a high degree of agglomeration but this is not always the case with this addition [22,24].

The analysis performed by XRF yields the relative concentration of oxides in the samples shown in Table 1. Since organic compounds are not detected by this technique they were quantified in terms of the loss on ignition. A high purity is obtained for silica fume, with a SiO_2 content of 96.3%, which is equal or higher than the values reported in recent publications for this kind of addition [15,22,23]. On the contrary, the synthesized silica nanoparticles have significantly lower silica content (87.7%) due to the amine functionalization that gives rise to a value of 12.4% for the loss on ignition. Finally, the results for CAP indicate that the oxides, basically SiO_2 , correspond to less than 31% of the sample composition and the rest must be basically assigned to the encapsulated organic compound (loss on ignition of 69.3%).

BET specific surface area values of the particles are also collected in Table 1. The value of 16.7 m^2/g obtained for silica fume is similar to that reported in the literature [15,23]. On the contrary, a slightly higher value (36.7 m^2/g) is obtained for NS, which is significantly lower than usual values found for silica nanoparticles in the literature. For example, Qing and co-workers reported a surface area equal to 160 m^2/g for the NS used in their work [23] and it is possible to find commercial products with values of up to 500 m^2/g (see for example Levasil 500/15%). Nevertheless, this result is in good agreement with the higher size of the amine functionalized particles comparing to other silica nanoparticles found in the literature as indicated previously. In the case of the microcapsules, it was necessary to wash them with acetone, in order to remove the epoxy, prior to performing the measurement. Otherwise, the

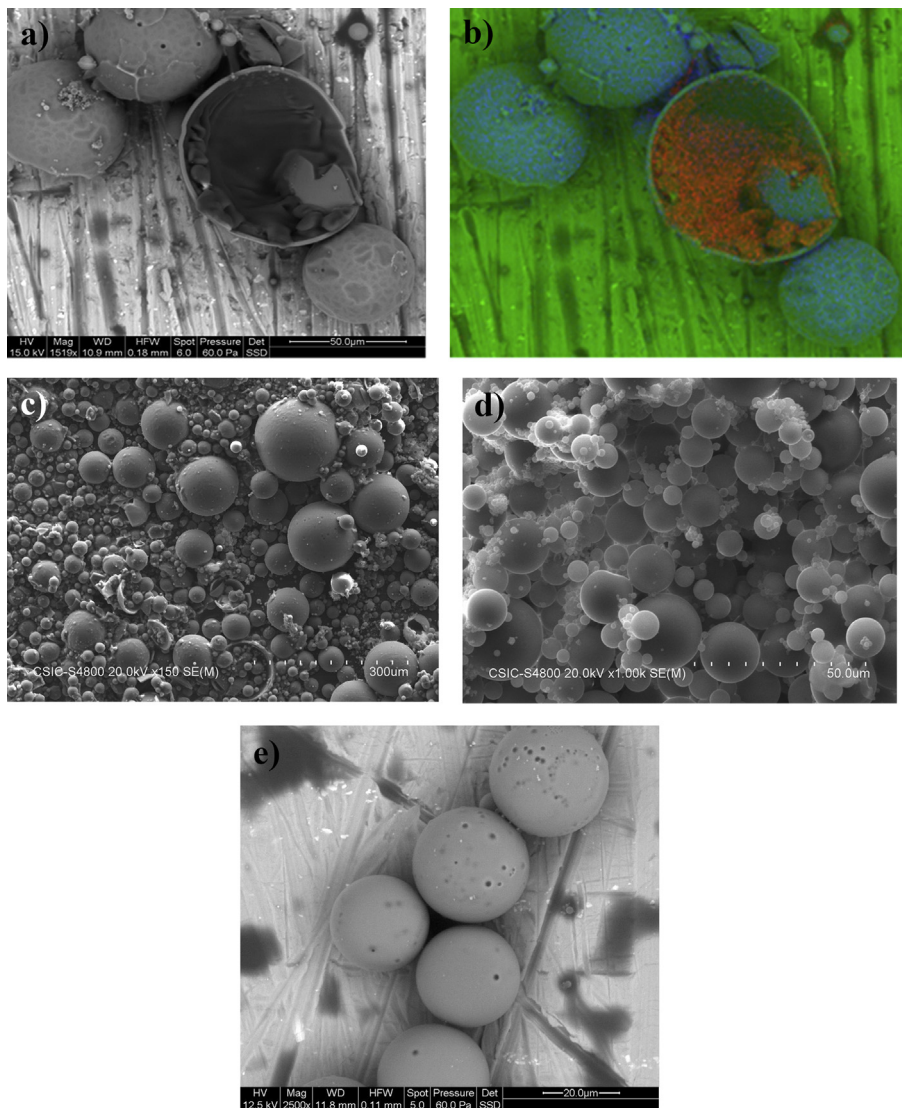


Fig. 1. SEM images of the epoxy containing microcapsules. a) Image of a broken microcapsule; b) Elemental analysis of image a) with Si signal in blue, C in red and Al in green; c), d) and e) Images with different magnification. (For interpretation of the references to colour in this figure legend, the reader is referred to the web version of this article.)

evaporation of the epoxy compound under vacuum would have made it impossible to obtain accurate results. The value obtained for the specific surface area of the empty microcapsules is $343.6 \text{ m}^2/\text{g}$. Although this value is comparable to that obtained by Ahn et al. ($377.7 \text{ m}^2/\text{g}$) [16], it is much larger than that for the other two additions studied in spite of their smaller particle size (see Figs. 1 and 3). This is a clear evidence of the porous structure of the silica shell resulting from the sol gel synthesis process [27–29]. In fact, assuming that silica microcapsules have a perfectly spherical surface and no porosity, the specific surface (SSA) area is given by the expression:

$$SSA = \frac{\text{Surface Area}}{\text{Mass}} = \frac{4\pi R_{Ext}^2}{\delta_{shell} \frac{4}{3}\pi (R_{Ext}^3 - R_{Int}^3)} = \frac{3R_{Ext}^2}{\delta_{shell} (R_{Ext}^3 - R_{Int}^3)} \quad (1)$$

where δ_{shell} is the density of the silica shell, and R_{Ext} and R_{Int} are the external and internal radius of the capsules respectively. Considering the SEM study, the microcapsules shown in Fig. 1a) with a particle size of $70 \mu\text{m}$ ($R_{Ext} = 35 \mu\text{m}$) and a shell thickness of $2 \mu\text{m}$ (i.e.

$R_{Int} = 33 \mu\text{m}$) may be regarded as representative of the average morphology of the microcapsules. Using such values and Equation (1) the density of the silica shell (δ_{shell}) would be $0,0015 \text{ g}/\text{cm}^3$. However, this value makes no sense because is comparable to that of the lightest silica aerogels, which are in fact highly porous materials. Furthermore, since the apparent density of the capsules, as determined by directly measuring their weight and apparent volume with a scale and a graduated cylinder (washed microcapsules) is about $0.3 \text{ g}/\text{cm}^3$, it is evident that the main contribution to the SSA comes from the porosity of the shell itself because the real density can never be smaller than the apparent one. Finally, the fact that no release of epoxy is observed by scanning electron microscopy suggests that tortuosity of the pore network is very high.

X-ray diffraction results of samples CAP, NS and SF are shown in Fig. 6. The smooth curves obtained make evident the amorphous nature of the three additions, in good agreement with the results available in the literature for silica fume (SF) and nanosilica (NS) [22,23]. The three diffractograms present a very wide peak with maximum intensity at an angle 2θ around 23° . This peak is slightly broader in the curves of the microcapsules (CAP) and the silica nanoparticles which might be due either to a slightly lower

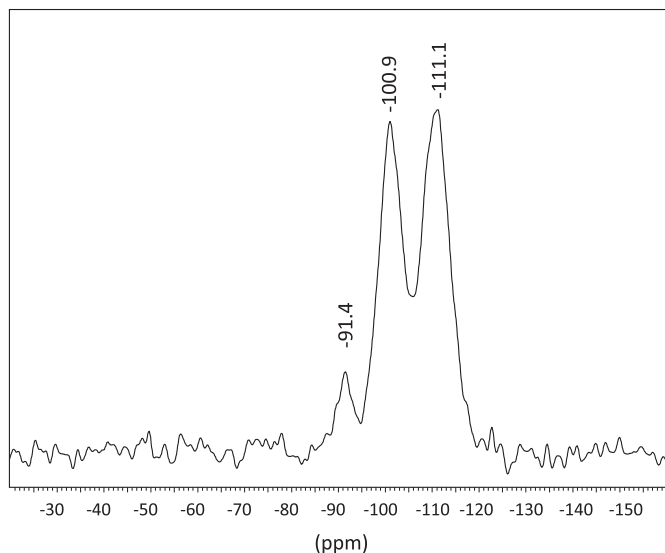


Fig. 2. ^{29}Si NMR of the epoxy containing microcapsules.

crystallinity of the particles synthesized in the laboratory or to a size effect. Although the microcapsules have diameters larger than SF particles, the fact that they are hollow spheres means that their effective size for diffraction is given by the thickness of the shell, which is much smaller. In the case of silica fume, a second diffraction peak is observed at 35.5° that corresponds to silicon carbide [19].

In order to complete the chemical characterization of the particles under analysis, their infrared transmission spectra are depicted in Fig. 7. In the spectrum of silica fume (SF) several broad bands may be observed. Those with minimum transmission at

1120 , 808 and 480 cm^{-1} correspond to vibrations of the Si–O bond in the amorphous silica (stretching, bending and rocking modes, respectively) where each silicon tetrahedron is connected to four neighbouring tetrahedra through Si–O–Si bridges [30]. The weak bands in 3450 and 1630 cm^{-1} correspond to vibrations of OH groups in water molecules that must be related in this case to water absorption in the hygroscopic KBr pellet.

Although the spectrum of NS is similar to that of SF, some interesting differences may be found. A stronger absorption in the bands due to OH groups is observed and a wider band associated to the stretching vibration of the Si–O bond with an additional peak at 958 cm^{-1} . This additional peak, together with that appearing at 572 cm^{-1} may be related to Si–O bond vibrations in tetrahedra with broken oxygen bridges, which means that one or more oxygen atoms are not linked to a neighbouring tetrahedron [31]. This is in good agreement with the ^{29}Si NMR spectrum of the NS in which the Q_3 and T_2 peaks are seen, due to silicon nuclei bound to OH groups. This contribution implies a less ordered structure compared to that of amorphous silica, as suggested by the X-ray diffractograms of Fig. 6. The expected absorption bands corresponding to the amine group are only detected around 3280 cm^{-1} and $2970\text{--}2940\text{ cm}^{-1}$, related to vibrations of the N–H bond and of the C–H bond, respectively. This slight influence of the amine in the spectrum of NS is coherent with the low concentration of the organic compound with respect to the silicon oxide in the particles.

The FTIR spectrum of the microcapsules encapsulating Epoxthin[®] (CAP) is also shown in Fig. 7 together with the spectrum of the silica spheres obtained after washing the CAP sample with acetone to remove the epoxy compound. In this case, the spectrum of CAP is mostly defined by the sharp peaks of the organic compound in good agreement with the composition obtained through XRF (Table 1). Nevertheless, the presence of the silica forming the shell of the capsule may be deduced by the decrease in transmittance observed in the wavenumber range

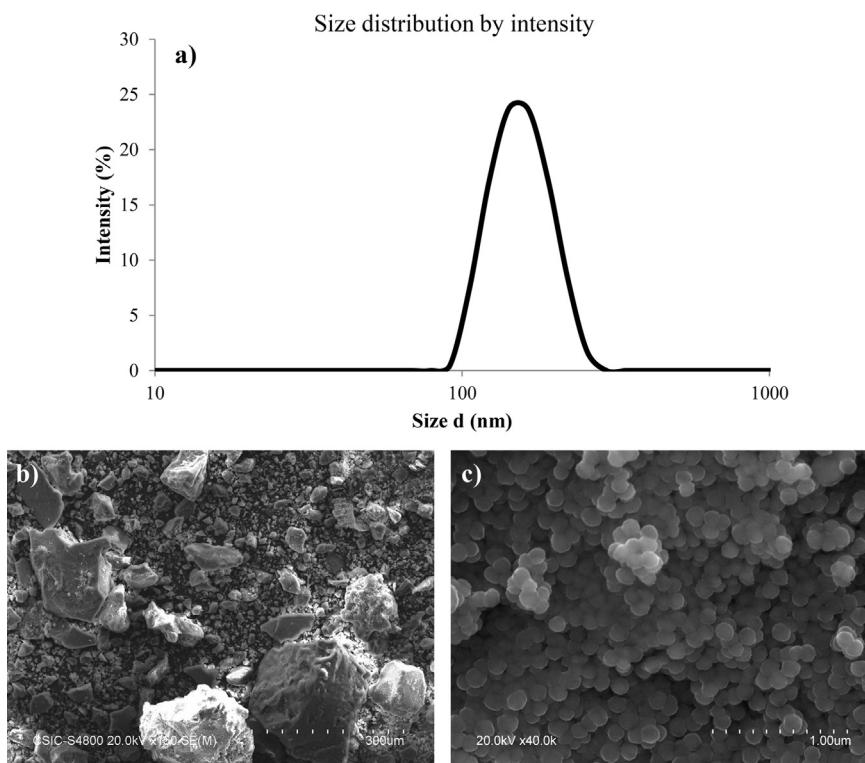


Fig. 3. a) Particle size distribution of NS characterized in the reaction dispersion by dynamic light scattering; b) and c) SEM images of NS with different magnification.

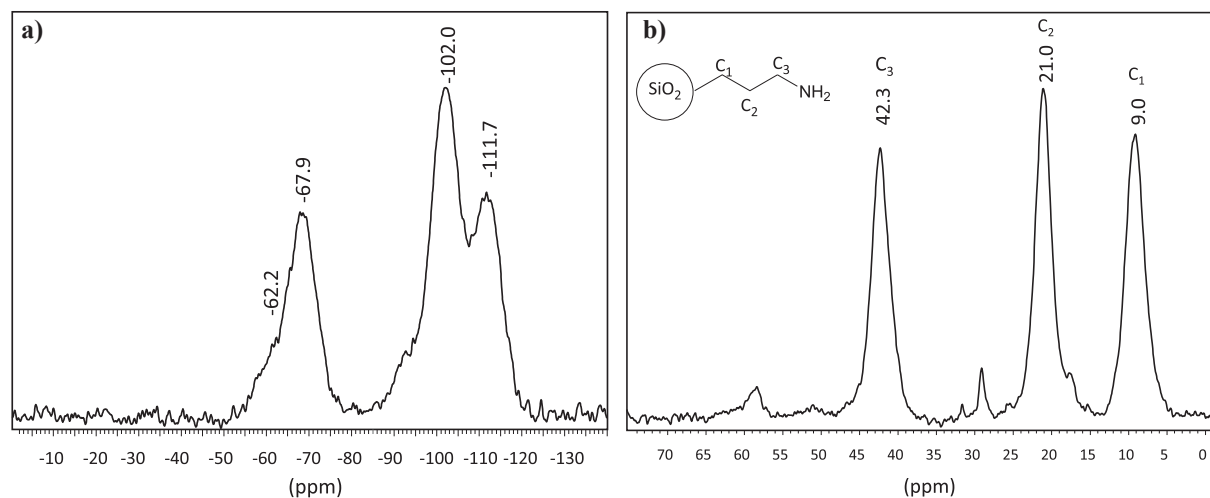


Fig. 4. ^{29}Si and ^{13}C solid NMR of the amine functionalized silica nanoparticles.

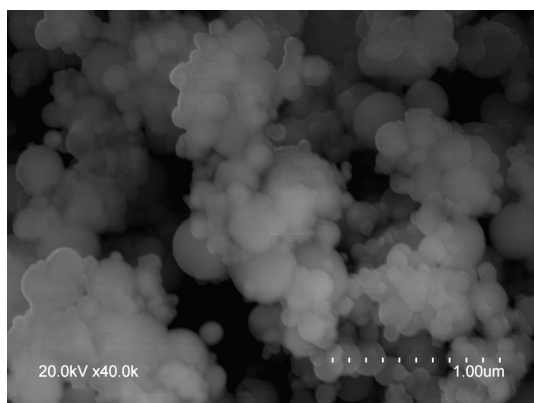


Fig. 5. SEM image of the commercial silica fume used in the study.

corresponding to the Si–O bond stretching band. It is interesting to note that the peak due to the oxirane ring can also be seen at 915 cm^{-1} , as noted by a square in Fig. 7. This indicates that the epoxide group did not react during the microencapsulation process and keeps intact for subsequent curing reactions. It is also interesting to note the presence of the peak at 958 cm^{-1} and 572 cm^{-1} already observed in NS and attributed to Si–O bonds with broken oxygen bridges, again in good agreement with the ^{29}Si NMR spectrum of the microcapsules.

3.2. Determination of pozzolanic activity

The epoxy containing microcapsules and the amine functionalized nanosilica studied in this work are intended to be used in the development of a smart self-healing concrete. Taking this into account, the microcapsules are made of silica in order to assure good compatibility with the cement paste. Similarly, the amine group has been functionalized on nanosilica due to its high pozzolanic activity for ensuring that the amine group will form part of the cementitious matrix once the nanosilica particles react with cement. In both cases, the amorphous character of the particles should improve the reactivity during hydration.

As a step further to confirm the proper behaviour of both particles within a cementitious matrix, their pozzolanic activity was studied by the accelerated method proposed by Sanchez de Rojas and co-workers [19]. This test will indicate the capability of the particles to react with the calcium hydroxide present in the cementitious matrix under hydration, to give rise to an enhancement of the formation of calcium silicate hydrate phase (C–S–H gel), responsible for the high mechanical strength of cement composites.

The results from the pozzolanic activity test of the three additions under study (Fig. 8) show that silica fume is less reactive at early ages than the other two additions. In particular, the amount of fixed lime after 1 day is almost 90% for NS and CAP and 82% for SF. Additionally saturation is not reached before 28 days for SF while it takes place after only 7 days for NS. These results are in good agreement with the data reported in the literature comparing nanosilica and silica fume and it has been related to the different chemical structure of both additions and to the higher specific

Table 1
Oxides composition, loss on ignition and BET specific surface area of epoxy containing microcapsules (CAP), amine functionalized nanosilica (NS) and commercial silica fume (SF).

| Addition | Oxides composition (%) | | | | | | | BET surface area (m^2/g) |
|----------|------------------------|--------------------------------|------|--------------------------------|------|--------------------------------|------|--|
| CAP | SiO₂ | Al ₂ O ₃ | CaO | | | | | L.I. |
| | 30.62 | 0.05 | 0.01 | | | | | 69.32 |
| NS | SiO₂ | | | | | | | L.I. |
| | 87.72 | | | | | | | 12.39 |
| SF | SiO₂ | K ₂ O | MgO | Fe ₂ O ₃ | CaO | Cr ₂ O ₃ | ZnO | L.I. |
| | 96.34 | 0.82 | 0.42 | 0.33 | 0.16 | 0.13 | 0.03 | 1.77 |

L.I. – Loss on ignition.

For the present study, the most interesting value regarding the composition of the samples is the percentage of silica, which is highlighted in bold.

^a After processing the sample as described in the text.

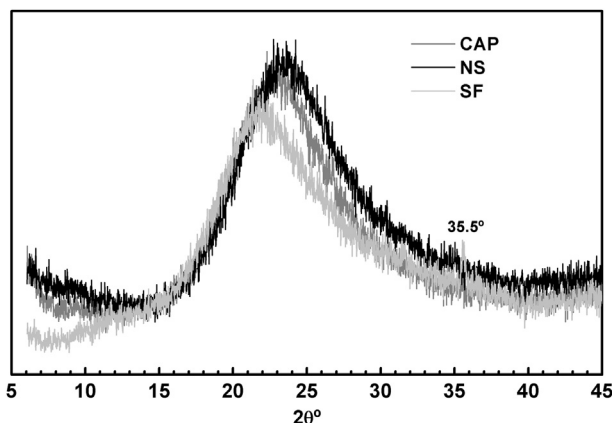


Fig. 6. X ray diffraction pattern of epoxy containing microcapsules (CAP), amine functionalized nanosilica (NS) and commercial silica fume (SF).

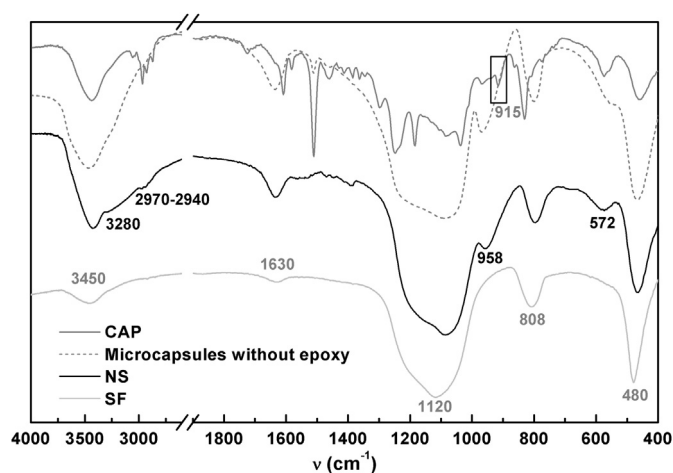


Fig. 7. Infrared absorption spectra of epoxy containing microcapsules (CAP), microcapsules without epoxy (obtained after washing a CAP sample with acetone), amine functionalized nanosilica (NS) and commercial silica fume (SF).

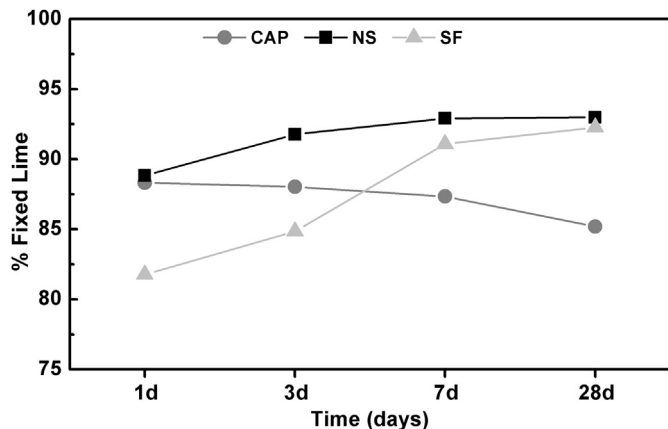


Fig. 8. Percentage of lime fixed by epoxy containing microcapsules (CAP), amine functionalized nanosilica (NS) and commercial silica fume (SF) in the pozzolanic activity test.

surface area of nanosilica [22,23]. For the case of the particles compared in Fig. 8, the analysis presented in Section 3.1 has shown that NS and CAP have Si–OH bonds, so that their pozzolanic

reaction must be quick. On the contrary, in the case of SF it is necessary a prior step for breaking the saturated Si–O–Si bonds from the surface and, as the energy of this bond is high, the process must be slower. Moreover, as NS has a specific surface area higher than SF (see Table 1), it is expected to show a higher reactivity.

Also interesting to note is that the amount of fixed lime at the end of the experiment is similar for NS and SF and considerably smaller for CAP. Lime fixation depends mainly on the amount of reactive silica of each addition. In the case of NS and SF the total amount of silica is 88 and 96 wt.% respectively while for CAP is only 36wt% (see Table 1). Assuming that the proportion of reactive to total silica in the three types of particles is not drastically different, this would explain why the maximum fixation level is lower for CAP than for the other two additions. In fact, the results suggest that all the reactive silica in the microcapsules is consumed within one day and the pozzolanic reaction cannot progress thereafter.

With respect to the liquid phase after the pozzolanic activity tests, the measured values of pH and conductivity are depicted in Fig. 9a) and b), respectively. In the case of the amine functionalized silica nanoparticles, the main effects are observed during the first three days, in which the clear decrease in pH and conductivity of the liquid phase is related to the incorporation of Ca^{2+} ions into the solid phase upon reaction with silica. A similar behaviour is observed for SF with a slower pozzolanic reaction that extends up to seven days. The high value of conductivity measured for SF at early ages may be related to its lower pozzolanic activity. These results are coherent with the values of fixed lime shown in Fig. 8 for these two additions. For the case of microcapsules, an almost constant value of conductivity up to 28 days is consistent with the values obtained for fixed lime percentage in the solid phase and indicates that Ca^{2+} incorporation into the solid phase does not progress with time. On the other hand, the continuous decrease of pH of the liquid phase observed in Fig. 9a) suggests that equilibrium has not been reached at the end of the test.

In order to better understand the behaviour of the silica microcapsules and to confirm their stability upon reaction with lime, the CAP sample as synthesized and after the pozzolanic activity test for 1 and 28 days has been further analyzed by FTIR and SEM. Fig. 10 collects the corresponding infrared transmission spectra. It is observed that, increasing the reaction time with the saturated lime solution produces an increase in the absorption within the range $1010\text{--}880\text{ cm}^{-1}$, highlighted by a dotted square and related to hydrate silicates. This behaviour confirms the C–S–H gel development due to the pozzolanic reaction.

SEM images of the sample CAP after the pozzolanic test are included in Fig. 11. In Fig. 11a) it is seen that the sample after 1 day of reaction is formed by a loose material and its morphology is defined by spherical microcapsules with a more amorphous phase between them. Fig. 11b) shows a zoom of the previous image in which microcapsules are seen in different states of reaction.

EDX spectra were obtained for several points of the sample considering well-defined spheres and well-reacted microcapsules. The resulting values of mean Ca/Si ratio and carbon atomic percentage for the two different morphologies are collected in Table 2. It is observed that the Ca/Si ratio is higher in the reacted (0.48) than in the complete spheres (0.30), suggesting that the Ca^{2+} ions have been mostly incorporated in the reaction products. Regarding the mean carbon content values, there is a contribution from the graphite layer on the sample surface and a higher dispersion in the results is observed. Nevertheless, a clearly higher content of this element was obtained in the reacted phase (69%) as compared to the spheres (43%) that could be related to the epoxy compound spread out from the reacted microcapsules.

Two different morphologies were found by the SEM analysis of sample CAP after the test for 28 days. Fig. 11c) shows the

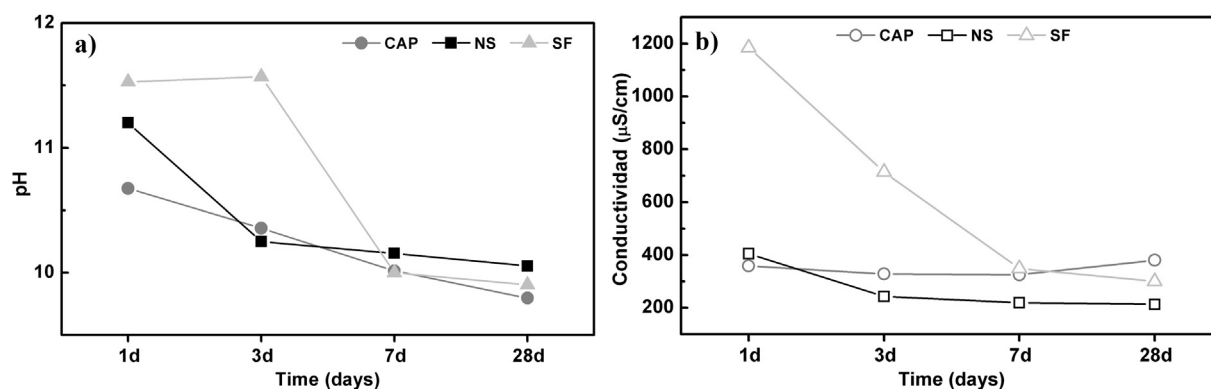


Fig. 9. pH values and conductivity of the liquid phase after the pozzolanic activity test on epoxy containing microcapsules (CAP), amine functionalized nanosilica (NS) and commercial silica fume (SF).

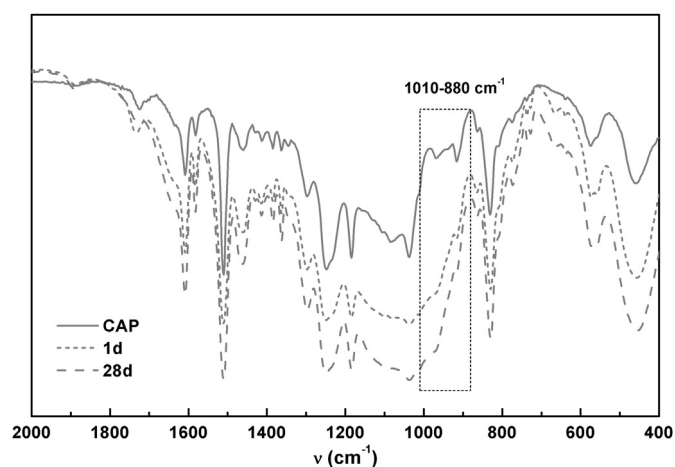


Fig. 10. Infrared transmission spectra of CAP as synthesized and after the pozzolanic activity test for 1 and 28 days.

characteristic aspect of one of these morphologies where a significantly denser structure is observed as compared to that after 1 day of reaction. Fig. 11d) shows a zoom of this amorphous phase, where it is observed that after the test for 28 days most of the capsules have completely reacted to give rise to a sponge-like structure. This morphology is similar to that observed for silica fume subjected to the same test [19].

Apart from the morphology previously described, other areas of the sample after 28 days of reaction have the aspect shown in Fig. 11e) and f). At low magnification (Fig. 11e)) these areas seem to be formed by a continuous phase, but upon zooming the structure is observed to be formed by agglomeration of well defined small spheres (Fig. 11f)).

The mean values of Ca/Si and atomic percentage of carbon obtained by EDX for the sponge-like structure in Fig. 11d) and the agglomerated spheres in Fig. 11f) are included in Table 2. The composition of the reacted spheres is similar at both ages of reaction, with a Ca/Si ratio around 0.50 and a carbon content of 69%. On the contrary, the Ca/Si value of the well-defined spheres is half the value obtained for 1d of reaction. This result may be due to a migration of calcium ions to the areas in which the internal parts of the capsules seem to be under pozzolanic reaction, thus demanding more calcium ions to form C–S–H-gel.

The results described indicate that the microcapsules have a pozzolanic activity that gives rise to the formation of a gel-like structure upon 28 days of reaction with a saturated lime solution.

The higher carbon content measured in this structure suggests the release of the epoxy compound as the microcapsules react to form the gel phase. Nevertheless, with increasing reaction time an agglomeration of intact small capsules in big structures with low Ca/Si ratio is also observed. This confirms the presence of a slight pozzolanic reaction also in these capsules, but the lower carbon content of these structures suggests that the epoxy compound remains stable within the capsules.

As a conclusion of this analysis it can be said that the microcapsules show pozzolanic activity, which is positive to assure the good compatibility with the cementitious matrix under hydration. Moreover, only a portion of the capsules degrade by reaction with the saturated lime solution and spread the epoxy compound they contain. The main part of the microcapsules remains stable during the test and assures a proper isolation of the epoxy compound. This result is important, as the stability of the microcapsules upon hydration of the cementitious matrix is mandatory for the success of the self-healing concrete.

Regarding the amine functionalized nanosilica particles, they show a high pozzolanic activity, similar to that of silica fume at 28 days of reaction and with behaviour with reaction time similar to that reported by other authors for silica nanoparticles. This is also an important result as it may be inferred that the NS addition within a cementitious matrix will improve the development of C–S–H gel. This gel phase must efficiently include the amine group initially bonded to the nanosilica, which was another condition for our innovative self-healing system to be reliable.

4. Conclusions

Two types of innovative additions have been synthesized for the production of smart self-healing cement based materials: amine functionalized silica nanoparticles (NS) and silica microcapsules filled with epoxy resin (CAP). Morphological characterization of the as-synthesized particles indicates they possess a proper morphology and size to be considered as additions to cement. They are amorphous and present a relatively high specific surface area, both properties positive to enhance their reactivity. Moreover, their chemical characterization proves the stability of the epoxy compound inside the silica microcapsules in CAP, as well as the presence of amine groups bonded to silicon atoms in the silica nanoparticles of NS. It is also important to note that, although the high specific surface area of silica microcapsules evidences an elevated porosity, no escaping of the epoxy resin is observed, suggesting an elevated tortuosity. These results are of prime importance as a guarantee that the components of the sealing systems are appropriate to be introduced in the cementitious matrix.

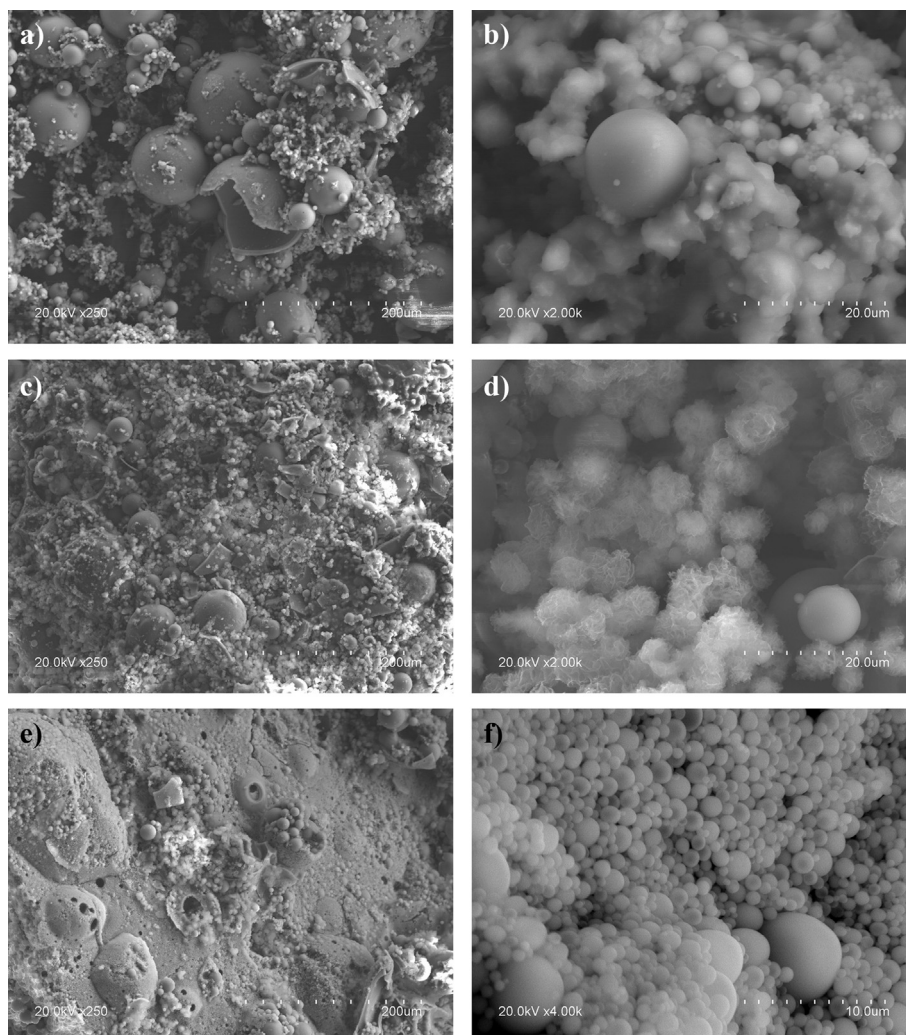


Fig. 11. SEM images of CAP after pozzolanic activity test. a) and b) after 1 day of reaction; c) and d) after 28 days: sponge-like structures; e) and f) after 28 days: agglomerated spheres.

Table 2

Mean values of Ca/Si and atomic percentage of C obtained by EDX in different morphologies observed in CAP after the pozzolanic activity test for 1 and 28 days.

| Morphology | Ca/Si | | | | Atomic percentage of C | | | |
|----------------------|-------|------|------|------|------------------------|----|------|----|
| | 1d | | 28d | | 1d | | 28d | |
| | Mean | SD | Mean | SD | Mean | SD | Mean | SD |
| Well-defined spheres | 0.30 | 0.04 | 0.16 | 0.02 | 43 | 6 | 35 | 6 |
| Reacted spheres | 0.48 | 0.08 | 0.50 | 0.10 | 69 | 3 | 69 | 5 |

Nevertheless, it is also fundamental to confirm that the self-healing system is stable upon the mixing and hydration processes of the cementitious materials. In order to check the latter, the pozzolanic activity test has been performed. Amine-functionalized nanosilica has proven to have a pozzolanic activity superior to that of the silica fume used as a reference. This suggests that NS addition will give place to the formation of amine functionalized C–S–H gel. By contrast, in the case of CAP, the results indicate that a good bond will be formed between the shell of the capsules and the matrix, but the silica capsules remain stable in a high proportion upon reaction with lime. This is important to ensure that the capsules will properly isolate the EPOTHIN[®] and they will break at the same

time as the matrix, liberating the epoxy resin throughout the cracks.

Acknowledgements

The authors would like to acknowledge to M.T. Vázquez and J.A. Sánchez, to the Service Unit of IETcc-CSIC and the Infrared Spectroscopy Service of ICMM-CSIC for their help in the experimental work and gratefully acknowledge the financial support of the Projects BIA2011-29234-C02-01 and PI2012-23.

References

- [1] S.R. White, N.R. Sottos, J. Moore, P. Geubelle, M. Kessler, E. Brown, S. Suresh, S. Viswanathan, Autonomic healing of polymer composites, *Nature* 409 (2001) 794–797.
- [2] Self-healing materials: an alternative approach to 20 centuries of materials science, in: Sybrand van der Zwaag (Ed.), *Springer Series in Materials Science Series*, vol. 100, 2007.
- [3] M. Rooij, K. Van Tittelboom, N. De Belie, E. Schlangen, *Self-healing Phenomena in Cement-based Materials. State-of-the-art Report of RILEM. Technical Committee 221-SHC: Self-healing Phenomena in Cement-based Materials*, 2013.
- [4] K. Van Tittelboom, N. De Belie, *Self-healing in cementitious materials – a review*, *Materials* 6 (2013) 2182–2217.
- [5] Z. Yang, J. Hollar, X. He, X. Shi, *Laboratory assessment of a self-healing*

- cementitious composite, *J. Transp. Res. Board* 2142 (2010) 9–17.
- [6] X. Wang, F. Xing, M. Zhang, N. Han, Z. Qian, Experimental study on cementitious composites embedded with organic microcapsules, *Materials* 6 (2013) 4064–4081.
- [7] F. Xing, Z. Ni, N.X. Han, B.Q. Dong, X.X. Du, Z. Huang, M. Zhang, Self-healing mechanism of a novel cementitious composite using microcapsules, in: *Proceedings of International Conference on Durability of Concrete Structures*, Hangzhou (China), November, 2008, pp. 195–204.
- [8] M.M. Pelletier, R. Brown, A. Shukla, A. Bose, Self Healing Concrete with a Microencapsulated Healing Agent. <http://energetics.chm.uri.edu/system/files/Self%20healing%20concrete%20-7-11.pdf>.
- [9] B.J. Blaiszik, S.L.B. Kramer, S.C. Olugebefola, J.S. Moore, N.R. Sottos, S.R. White, Self-healing polymers and composites, *Annu. Rev. Mater. Res.* 40 (2010) 179–211.
- [10] H. Zhang, J. Yang, Development of self-healing polymers via amine-epoxy chemistry: I. Properties of healing agent carriers and the modelling of a two-part self-healing system, *Smart Mater Struct.* 23 (2014) 065003, <http://dx.doi.org/10.1088/0964-1726/23/6/065003>.
- [11] T. Yin, M.Z. Rong, M.Q. Zhang, G.C. Yang, Self healing epoxy composites—preparation and effect of the healant consisting of microencapsulated epoxy and latent curing agent, *Compos Sci. Technol.* 67 (2007) 201–212.
- [12] D.S. Xiao, M.Z. Rong, M.Q. Zhang, A novel method for preparing epoxy-containing microcapsules via UV irradiation-induced interfacial copolymerization in emulsions, *Polymer* 48 (2007) 4765–4776.
- [13] H. Jin, C.L. Mangun, D.S. Stradley, J.S. Moore, N.R. Sottos, S.R. White, Self-healing thermoset using encapsulated epoxy-amine healing chemistry, *Polymer* 53 (2012) 581–587.
- [14] C.J. Barbé, L. Kong, K.S. Finnie, S. Calleja, J.V. Hannah, E. Drabarek, D.T. Cassidy, M.G. Blackford, Sol-gel matrices for controlled release: from macro to nano using emulsion polymerization, *J. Sol-gel Sci. Technol.* 46 (2008) 393–409.
- [15] R. Siddique, Utilization of silica fume in concrete: review of hardened properties, *Resour. Conserv. Recy* 55 (2011) 923–932.
- [16] B.Y. Ahn, S.I. Seok, I.C. Baek, S.I. Hong, Core/shell silica-based in-situ microencapsulation: a self-templating method, *Chem. Commun.* (2006) 189–190.
- [17] W. Stöber, A. Fink, E. Bohn, Controlled growth of monodisperse silica spheres in the micron size range, *J. Colloid Interface Sci.* 26 (1968) 62–69.
- [18] G. Berriozabal, Síntesis, funcionalización y caracterización de nanopartículas de óxidos de silicio, zinc y titanio, Ph.D. Thesis, UPV-EHU, 2011.
- [19] M.I. Sanchez de Rojas, J. Rivera, M. Frias, Influence of the microsilica state on pozzolanic reaction rate, *Cem. Concr. Res.* 29 (1999) 945–949.
- [20] I. Kalzakorta, E. Erkizia, Study on the effect of sol-gel parameters on the size and morphology of silica microcapsules containing different organic compounds, *Phys. Stat. Sol. C* 7 (11–12) (2010) 2697–2700.
- [21] V.S. Ramachandran, J.J. Beaudoin, *Handbook of Analytical Techniques in Concrete Science and Technology*, Noyes Publications/William Andrew Publishing, 2001, pp. 646–647.
- [22] P. Hou, S. Kawashima, D. Kong, D.J. Corr, J. Qian, S.P. Shah, Modification effects of colloidal nanoSiO₂ on cement hydration and its gel property, *Compos. Part B* 45 (2013) 440–448.
- [23] Y. Qing, Z. Zenan, K. Deyu, C. Rongshen, Influence of nano-SiO₂ addition on properties of hardened cement paste as compared with silica fume, *Construct Build. Mater* 21 (2007) 539–545.
- [24] B.W. Jo, C.H. Kim, G. Tae, J.B. Park, Characteristics of cement mortar with nano-SiO₂ particles, *Construct Build. Mater* 21 (2007) 1351–1355.
- [25] A. van Blaaderen, A. Vrij, Synthesis and characterization of monodisperse colloidal organo-silica spheres, *J. Colloid Interf. Sci.* 156 (1993) 1–18.
- [26] G. Berriozabal, Y.R. de Miguel, Synthesis and characterization of silica nanoparticles bearing different functional groups obtained via two-stage method, *Phys. Stat. Sol.* 11–12 (2010) 2692–2696.
- [27] J. Brinker, G.W. Scherer, *Sol-gel Science: the Physics and Chemistry of Sol-gel Processing*, Gulf Professional Publishing, 1990.
- [28] K.S. Finnie, J.R. Bartlett, C.J.A. Barbé, L. Kong, Formation of silica nanoparticles in microemulsions, *Langmuir* 23 (2007) 3017–3024.
- [29] A.J. Bush, R. Beyer, R. Trautman, C.J. Barbé, J.R. Bartlett, Ceramic micro-particles synthesised using emulsion and sol-gel technology: an investigation into the controlled release of encapsulants and the tailoring of micro-particle size, *J. Sol-gel Sci. Technol.* 32 (2004) 85–90.
- [30] M. Handke, W. Mozgawa, M. Nocun, Specific features of the IR spectra of silicate glasses, *J. Mol. Struct.* 325 (1994) 129–136.
- [31] P. Yu, J. Kirkpatrick, B. Poe, P.F. McMillan, X. Cong, Structure of calcium silicate hydrate (C-S-H): near-, mid-, and far-infrared spectroscopy, *J. Am. Ceram. Soc.* 82 (1999) 742–748.